Session 4 - Hot Film Measurements

EXPERIMENTAL INVESTIGATION WITH HOT-FILM GAUGES MOUNTED ON A SINGLE BLADE IN TRANSONIC FLOW

C.A. Poensgen & H.E. Gallus

RWTH Aachen, Germany

H.D. Schulz

KKK Frankental, Germany

K.D. Broichhausen & T. Schroeder

MTU München, Germany

Abstract:

Results of measurements with hot-film gauges on transonic compressor blades are extremely difficult to interpret because of the complexity of the local flow pattern. The fluctuations of shock waves and unsteady shock boundary layer interaction lead to probe signals which are ambiguous. Therefore, the output signals of hot-film probes mounted on a single airfoil in a transonic linear cascade were investigated, and the results were compared to results obtained by other measuring techniques. Thus, a method has been developed that allows the designer to interpret characteristic signals from hot-film probes.

Introduction:

The development to higher pressure ratios in axial compressors leads to higher axial flow velocities. Therefore, in modern maschines the outer parts of compressor stages operate in transonic or supersonic flow. The flow around transonic compressor blades is dominated by a shock system, which builds up somewhere inside the blade passage. Mostly this shock system is unsteady and connected to shock- boundary layer interactions. Small changes of incidence have a great influence on the location and intensity of the shock system. Since strong shocks lead to high losses, it is very important to predict the location of the shock system as accurate as possible.

In order to test the quality of a newly designed profile, the blade has to be investigated experimentely. The hot-film anemometry is a very appropriate tool for measuring the state of the blade boundary layer. With this technique, unsteady measurements are possible, and a high number of sensors can be placed on the surface of the airfoil. In contrary to flat pressure transducers, the hot-film anemometry allows to use at least three times more sensors, and the distortion of the blade surface due to the sensors is much smaller. But the presence of an unsteady shock system, boundary layer transition and flow separation leads to ambiguous signals, and it is very difficult to interpret the results obtained by hot-film anemometry. The goal of the herein described investigation is to give a tool to the experimentalist for better examination of hot-film signals from transonic compressor blades.

Test Facility

The investigations have been carried out in a linear transonic cascade shown in Fig.1. The flow enters from the air supply system into a large distribution chamber, where total pressure and total temperature are measured. The flow is accelerated through a nozzle and enters into the test bed. In order to simulate conditions which are typical for the transonic compressor flow, a suitable variation of Machnumber, Reynoldsnumber and incidence should be possible. The test facility provides a continues air flow up to inlet Machnumbers of 0.95 and Reyoldsnumbers of up to $1.8\ 10^6$.

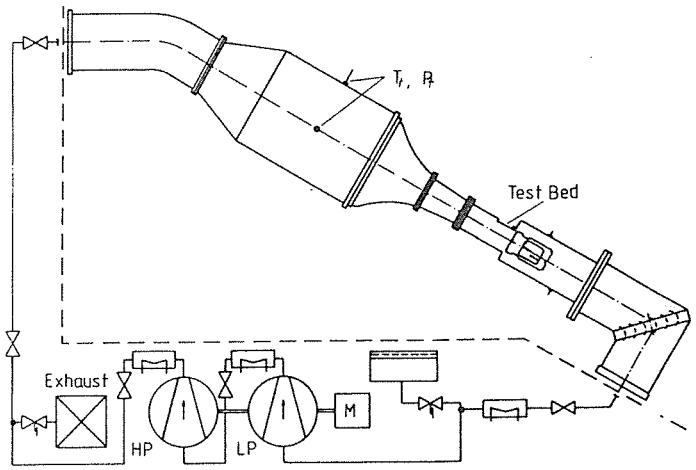

Fig. 1: Rectangular Test Facility

Fig. 2 shows the cross section of the test bed for tests with a single airfoil. The sidewalls (No.2 in Fig. 2) are perforated to avoid shock reflections and adjustable tailboards (No. 3 in Fig. 2) are incorporated to remove the side-wall boundary layers. The airfoil is mounted on a rotating disc (Fig. 3) to adjust incidence angles, and thus typical compressor shock configurations can be produced. Of great interest is the investigation of small shock systems in flows with zero incidence and strong shock systems in loaded flows, as well as their interaction with the profile boundary layer.

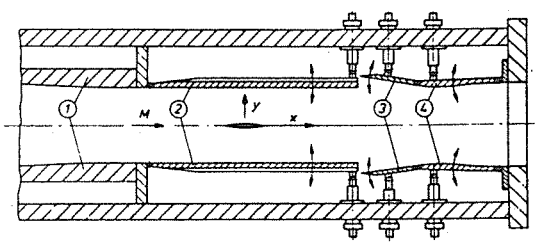

Fig. 2: Cross Section of the Test Bed

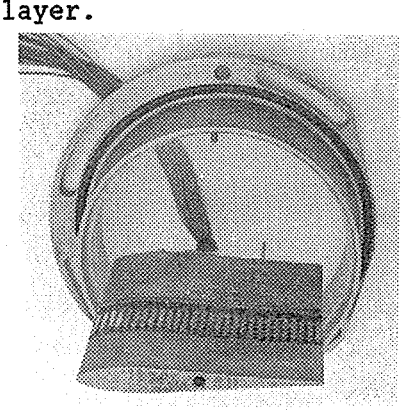

Fig. 3: Blade Traversing Mechanism

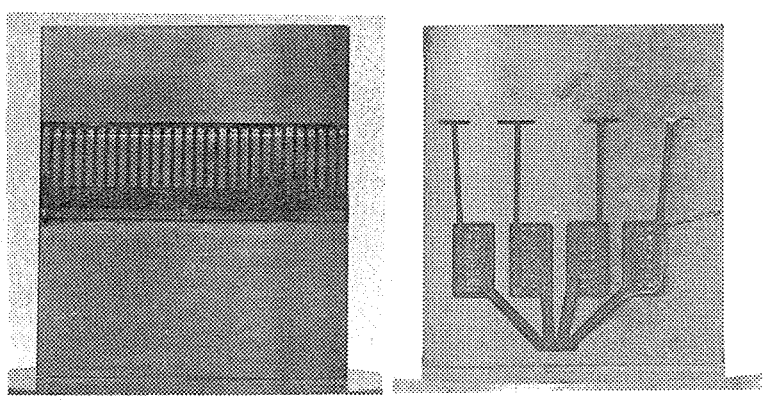

Fig. 4: Test Blade with mounted Hot-Film Sensors

Data Aquisition and Test Program

The task of the herein described investigation is to develop a method to aid the experimentalist to interprete hot-film signals in transonic flow. Therefore, various measuring techniques have been used parallel to the hot-film measurements for comparison.

The hot-film sensors are designed and produced by MTU München, and they are mounted on the upper side of the test blade (Fig. 4). Small cables are soldered to the leads of the hot-film sensors, which are introduced through a hollow bolt in the side-walls. All cables are mounted in groves filled up with resin, and there is no distortion to the airfoil surface. A common back lead has been used to reduce the number of cables. The major drawback of this application is that only one sensor can be operated at a time. Thus, two-channel Fourier analysis cannot be applied, and the cross correlation function, which gives information about the development of macroscale structures inside the boundary layer cannot be computed.

The scheme of the hot-film data aquisition is shown in Fig. 5. The hot-film sensors are connected to a DISA M55 anemometer system. The output voltage is recorded via an IBM-AT compatible computer, which is equipped with a high speed analog-digital converter with a resolution of 12 bits. As it is very inpractible to calibrate hot-film sensors, only the output voltage has been used for these investigations. Therefore, only a qualtitative analysis is possible. Typical flow phenomena, like for example laminar turbulent transition, lead to typical output signals of the hot-film sensors (Schulz and Gallus (1989), Schroeder (1989)). Beside the analysis of the real-time signal, the time-averaged output voltage and the RMS-voltage made dimensionless by the zero output voltage are of interest (equ. 1 and 2). To determine the time averaged anemometer output voltage, 2000 values were taken with a sampling frequency of 1 kHz. The determination of the RMS values is dependent on the corner frequency of the hot-film-anemometer system and the Shannon Factor to prevent alising effects. Thus, the sampling frequency was set to 80 Khz.

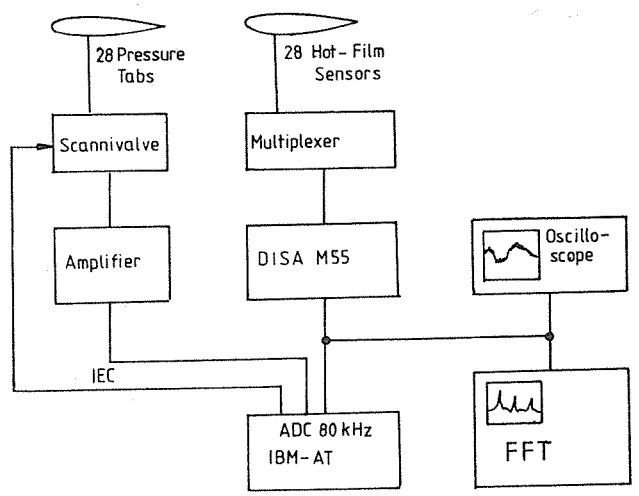

Fig. 5: Hot-Film Data Aquisition

$$\bar{u} = \frac{1}{T}\int_0^T u(t)\,dt \qquad (1)$$

$$u_{RMS} = \sqrt{\frac{1}{T}\int_0^T u^2(t)\,dt} \qquad (2)$$

Even though two channel Fourier analysis could not be applied, the signals are recorded by a NICOLET Fourier analyser, and at least the frequency spectra of the output signal were obtained.

In contrary of DANTEC's hot-film sensors, the MTU sensors are not coated with silicon. Thus, the MTU sensors have a high dynamic resolution with a corner frequency of 11 kHz. But there is a high risk of sensor damage due to particles in the transonic flow mainly in the region around the leading edge. During operation the MTU Sensors showed a good durability with respect to time. Fig. 7 shows the zero output voltages of the hot-film sensors for four different times within three months. All variations are within a range ±0.1 [V]. The first five sensors around the leading edge though broke, and

unfortunately no reliable data could be obtained there.
The following additional measurements have been taken for com-parison with the hot-film data:

- The location of the shock boundary layer development and boundary layer separation are visualized using the well known Schlieren technique.
- The pressure, respectively the Machnumber distribution were determined using a test blade with 28 pressure tabs along its cord. The results of these measurements have been used as input data to a numerical boundary layer computation. The code is based on the theory of McNally (1970), and the location of the laminar separation bubble is obtained by a method presented by Roberts (1975). Thus, an estimation of the boundary layer development can be found. Boundary layer transition and laminar separation have a great influence on the hot-film output signals. As laminar separation is located near the shock systems, the hot-film signals contain both information as it will be shown later in this paper.

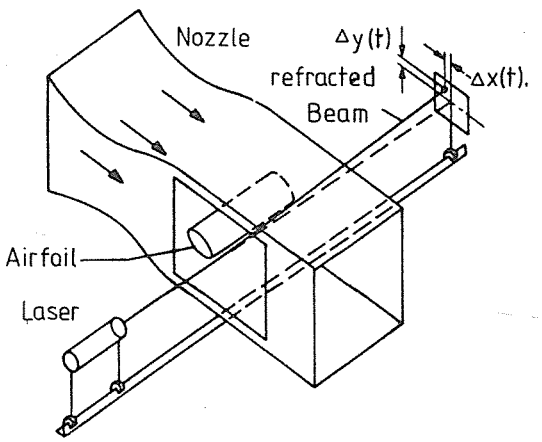

Fig. 6: Schematic Scetch of the Laser Density Gradient Technique

- The laser-density gradient measuring method (LDG) has been developed by Drees (1981) and is described by Broich-hausen at al. (1983) (Fig. 6). This method bases on Schlieren optics and is well suited to investigate the unsteady oscillations of shocks, pro-file wakes and vortices shed off a blunt trailing edge. In the herein described investi-gations, the laser beam was traversed parallel to the blade surface in cordwise direction with a distance of 1 mm above the blade surface. Thus, the fluctuations (periodic and random) of the shock system are determined, and reference data is obtained for comparison with the output signals of the hot-film anemometer.

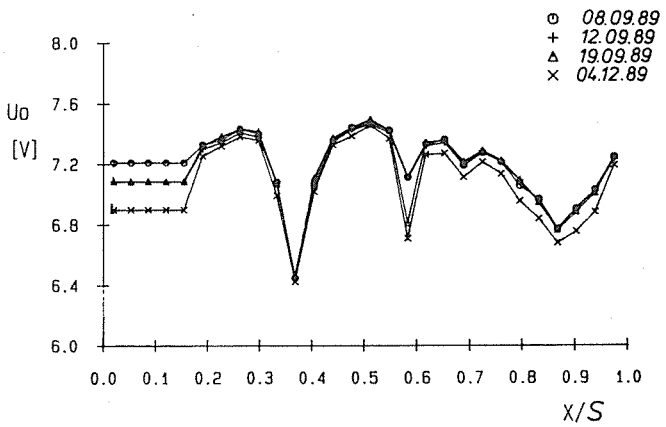

Fig. 7: Alterning Process of Hot-Film Sensors over Three Months.

Two typical compressor operation conditions were established with inlet Machnumbers of Ma_1 = 0.717 and Ma_1 = 0.737. For each Machnumber the flow angle to the blade was set to 1°, 2°, 3° and 4° incidence, respectively. All above described measurement techniques were applied in these tests, and the results are described in the following section.

Results and Discussion

Fig. 8 shows photographs taken with Schlieren optics of the flow around the isolated airflow under investigation. For the test case with zero incidence (Fig. 8a), a weak shock system is present at the upper and lower surface. The typical λ-structure can be seen. With increasing incidence angle, the shock becomes stronger and moves further downstream (Fig. 8b). Upstream of the

shock, compression waves are visible, which are reflected along the shock surface. They indicate an increase in pressure along the blade surface inside the profile boundary layer (for details see Delery at al. 1986). With incidence, the boundary layer becomes more loaded. For the highst loaded test case (3° incidence, not shown here) the boundary layer separates.

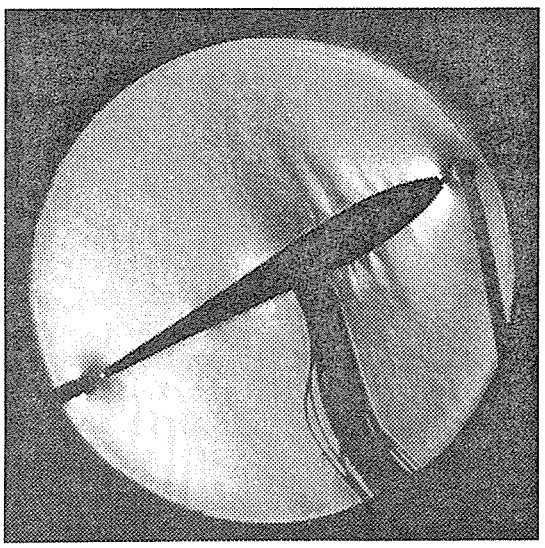

Fig. 8a: Schlieren Traces of the Shock System with $Ma_1 = 0.718$, $\alpha = 0°$

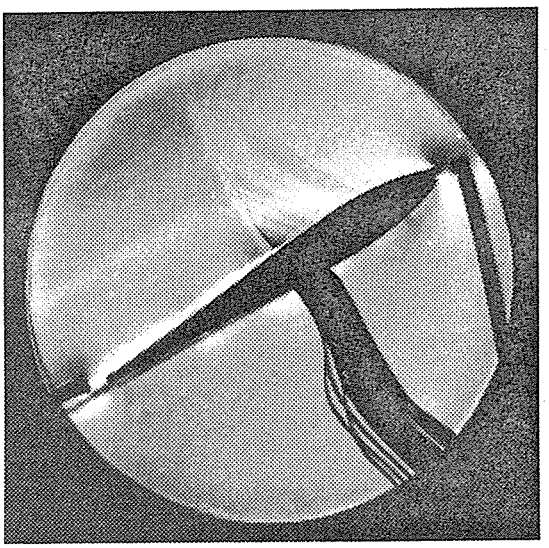

Fig. 8b: Schlieren Traces of the Shock System $Ma_1 = 0.718$, $\alpha = 2°$

The nondimensional pressure distributions for an inlet Machnumber of 0.717 are shown in Fig. 9. The resulting isentropic Machnumber distributions from these pressure measurements are shown in Fig. 10. Around the leading edge there is a strong expansion of the flow (labeled No. 1 in Fig. 9). At about 25% chord the pressure increases again (labeled No. 2 in Fig. 9). Upstream of the shock system the pressure curve flattened (nearly constant) which indicates a laminar separation bubble (labeled No. 3) (Henne (1989), Delery (1986)). The great increase in pressure (labeled No. 4) is directly related to the shock. The length of the separation bubble increases with incidence and thus with the strenght of the shock.

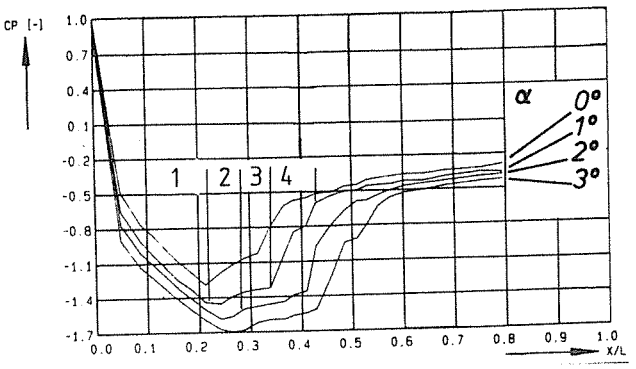

Fig. 9: Pressure Distribution Along the Blade Chord $Ma_1 = 0.718$, $\alpha = 0°, 1°, 2°, 3°$

Based on the Machnumber distribution (Fig. 10), the boundary layer can be numerically calculated according to the theory of McNally (1970). Using the separation criteria of Robers (1975), a laminar separation bubble was found. Thus the existence of laminar separation upstream of the shock is indicated by the pressure distribution and the numerical boundary layer investigation.

The time averaged DC-signal has been determined by averaging 2000 values recorded with a sampling of 1 kHz (equ. 1). Fig. 11 shows the chordwise distribution of the time averaged voltage for all points of operation. The

signal distributions of the sensors are very similar. Comparing these plots to the results from the Schlieren measurements, it is apparent that the location of the shock cannot be uniquerocally identified by the DC hot-film signals. For the test case with 3° incidence, the boundary layer separates downstream of the shock. Thus, the heat transfer from the hot-film into the flow decreases, which results in a decrease of the DC output voltage of the hot-film signal. This is shown clearly in Fig. 11.

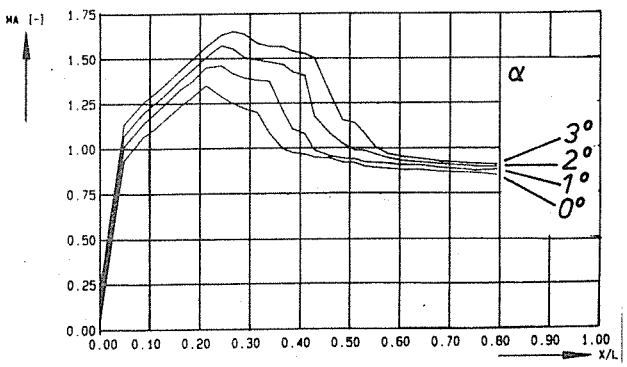

Fig. 10: Distribution of Machnumber Along Blade Chord Ma_1 = 0.717, α = 0°, 1°, 2°, 3°

There are several reasons why the time-averaged hot-film output voltages do not reveal the typical flow structures. The mean output voltage is dependent on the free-stream velocity as well as on the thickness of the boundary layer and also whether the boundary layer is laminar or turbulent. Downstream of the shock in the test case with zero incidence, the distribution of the Machnumber indicates lower flow velocities. Thus, one would expect to find lower time-averaged output voltages from the hot-film sensors. But the higher level of turbulence, and the thickening of the boundary layer leads to an enhanced heat flux from the sensors into to boundary layer, so that the output voltage remains nearly constant. The turbulent boundary layer downstream of the shock equals the influence of the lower velocity on the hot-film output voltage. Therefore in this case, the conclusions, which can be drawn from the time-averaged hot-film output voltage on the flow structure are rather poor.

A comparison between hot-film RMS-output voltage and the dimensionless pressure distribution is shown in Fig. 12. At all measurements, there is an increase of the hot-film RMS-voltage just upstream of the shock location. The maximum value of the RMS-voltage is located at the shock position, but the increase of the RMS-voltage starts further upstream. This effect might be due to the existence of the laminar separation bubble, which causes a higher turbulence level. For the higher loaded test cases, the maximum peak of the RMS-output signal is located at the shock position. Here, the Schlieren photographs show a sudden increase in boundary layer thickness, which indicates a turbulent boundary layer separation. Therefore, the RMS-voltages measured downstream of the shock remains at a high level at the 3° incidence test case, corroborating the turbulent boundary layer separation in this test case.

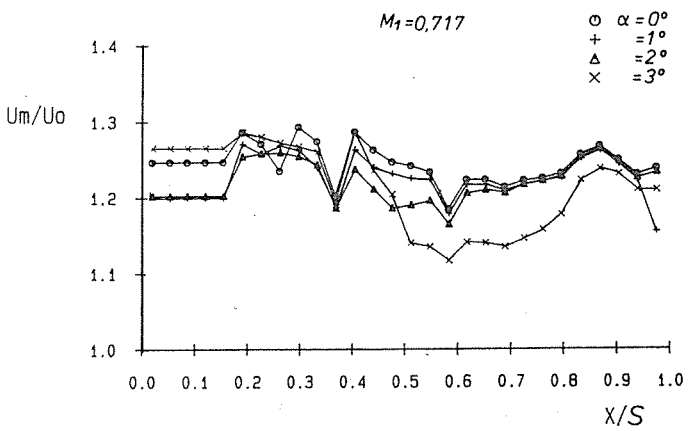

Fig. 11: Chordwise distribution of the Hot-Film Averaged DC Signal (Ma_1 = 0.718)

The location of the shock can be determined regarding the RMS- output voltage of the hot-film sensors. Due to the structure of the boundary layer beneath

the shock, and due to the unsteady shock fluctuations, the RMS-output voltage of the hot-film sensors increase and give a clear indication of the shock location. This is independent of whether the shock oscillates or is nearly steady. Though the extent of the separated boundary layer downstream of the shock can be estimated, the signals do not allow to draw any conclusions on the existence of a laminar separation just upstream of the shock location. Here all the above described effects superimpose the hot-film output signal, and therefore the laminar separation is not distinguishable.

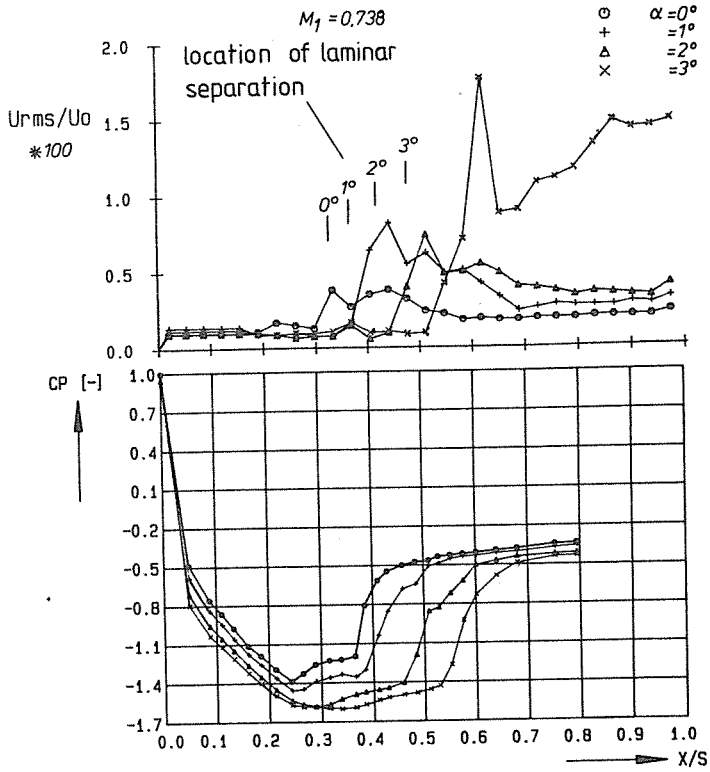

Fig. 12: Distribution of the Dimensionless RMS Voltage of the Hot-Film Along the Chord $Ma_1 = 0.717$

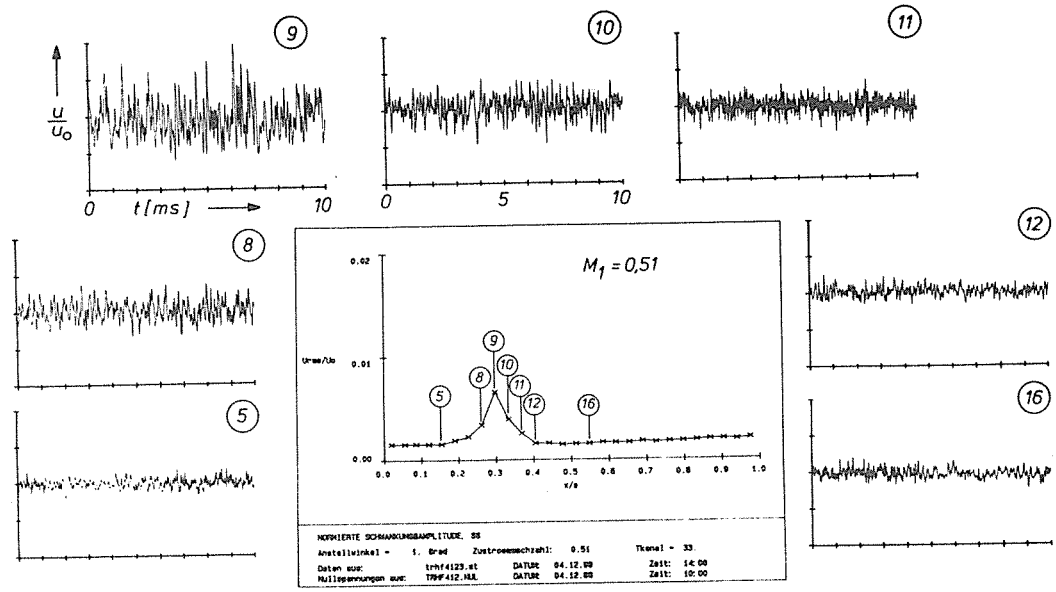

Fig. 13: Development of the Real-Time Signal and RMS Signal with Chord at $Ma_1 = 0.51$

The hot-film real-time signals in transonic flow do not indicate the flow structure as clearly as it can be seen in subsonic flow. For comparison, Fig. 13 shows the real-time traces and the development of the RMS-signal with chord for subsonic flow (i.e. $Ma_1 = 0.51$). Here, the laminar turbulent transition process is clearly visible.

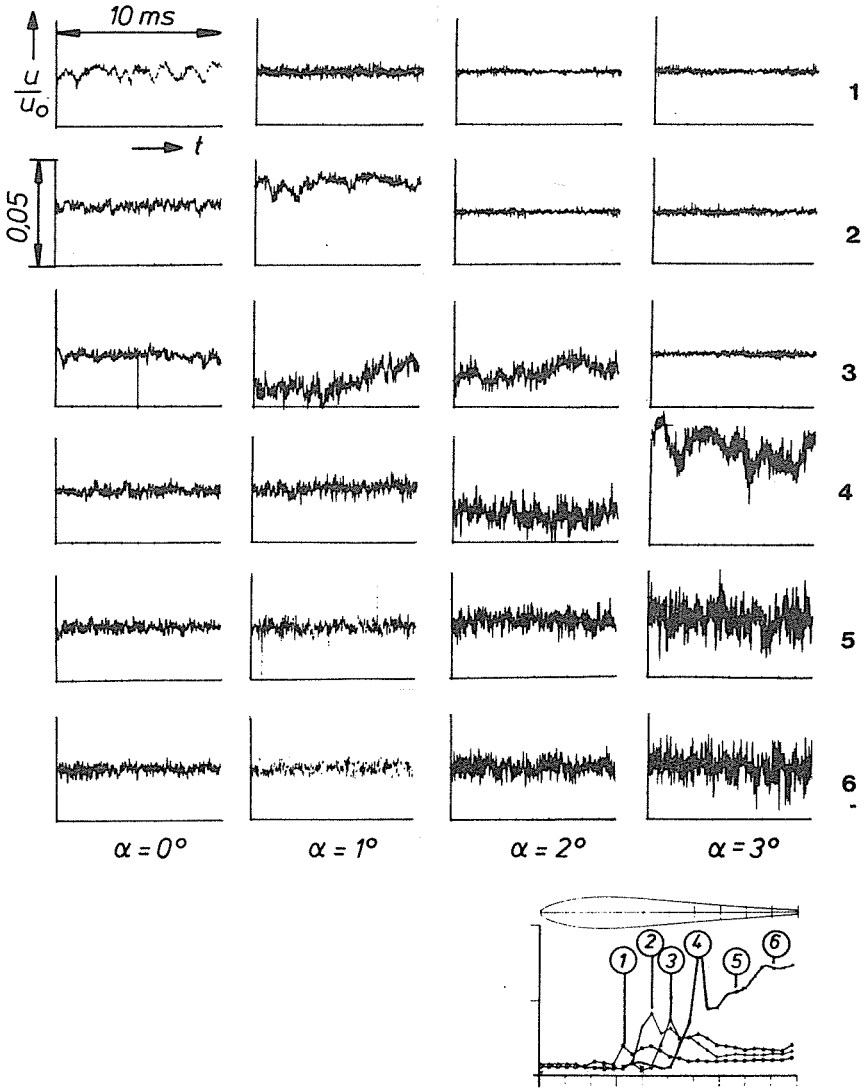

Fig. 14: Real-Time Signals at Ma_1 = 0.738 for all Points of Operation

Some real-time traces from the hot-film measurements for different points of operation are given in Fig. 14. The signals indicate laminar, turbulent and separated boundary layers. The location of the shock can be seen in the plots showing a lower frequent distortion (plot no.1 for α = 0°, plot no. 2 for α = 1°, plot no. 3 for α = 2° and plot no. 4 for α = 3° incidence). Regarding the plots at location 6, the unsteadiness is increasing. While the plots for the zero incidence test case here indicate a typical turbulent boundary layer, the plots corresponding to the 3° incidence test case show flow separation.

Considering the information obtained from the RMS-values, no additional insights are made available by the hot-film real-time traces. In transonic flow, the transition process is mostly in-fluenced by the shocks, which generally dominates the real-time signals. However, if the shock is unsteady, the oscillation of the shock is displayed in real-time signal by a low frequent oscillation, which could be useful for monitoring the shock location on an oscilloscope.

Comparison of Hot-Film Measurements and Results from the Laser-Density-Gradient Technique

The signals from the hot-film sensors are compared to those obtained by the LDG technique. The laser beam was traversed 1 mm above the blade surface along the chord. The density gradients refract the laser beam. The deviation of the laser beam is detected by a photocell, which can resolve in two axes (see Fig. 7).

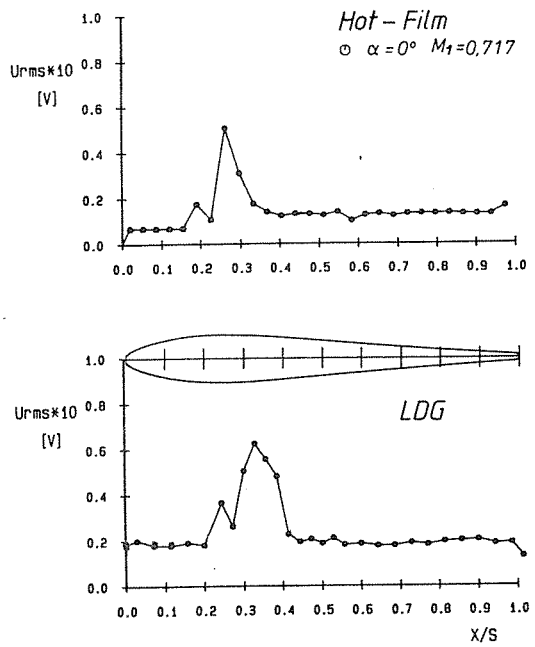

Fig. 15: Comparision of the Dimensionless Averaged RMS Voltage obtained with LDG- and Hot-Film Technique at Ma_1 = 0.717 and α = 0°

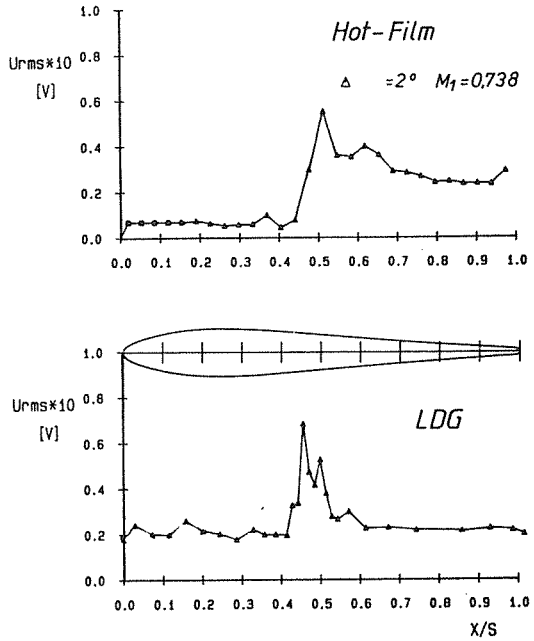

Fig. 16: Comparision of the Dimensionless Averaged RMS Voltage obtained with LDG- and Hot-Film Techniques at Ma_1 = 0.738 and α = 2°

A comparison of the RMS-voltage signals obtained with the LDG technique with those obtained by hot-film measurements is shown in Figs. 15 and 16. Regarding the Schlieren photographs, the location of the shocks is very well detected by the hot-film signal and the LDG measurements.
For the lower loaded test case (Fig. 15), the LDG measurements detect smaller density fluctuations at the leading edge of the lambda shock, and higher fluctuations at the trailing edge of the shock. While the LDG realy picks up the shock itself, the hot-film is receptive to the state of the boundary layer and therefore displays also the upstream influence of the shocks, which has been addressed above in this paper.

For the higher loaded test case with 2° incidence (Fig. 16), the results from the LDG measurements show a double peak at nearly the same location the hot-films exhibit a large increase in RMS-values. Downstream of the shock, the RMS-signals from the LDG measurements decrease to the same level they have upstream of the shock. The higher RMS-values of the hot-film signals give additional information about the degree of turbulence inside the boundary layer, which might be separated as can be concluded from the Schlieren photographs.

The frequency analysis of the output signals from the LDG- and hot-film measurements shows three characteristic frequencies (510 hz, 755 Hz and 970 Hz), which indicate the periodic unsteadiness of the shock. The periodic fluctuation of the shock does not result into a single peak, but rather in a

broad band amplification in the frequency domain, i.e. the peak frequency varies about ±10 Hz.

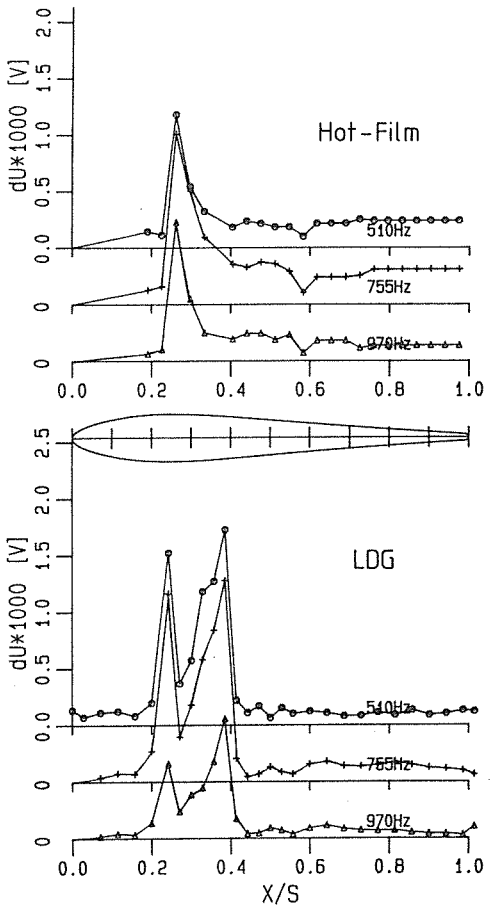

Fig. 17: Comparision of the Frequency- Spectras out of Hot-Film Measurements with LDG Measurements at Ma_t = 0.738 and α = 0°

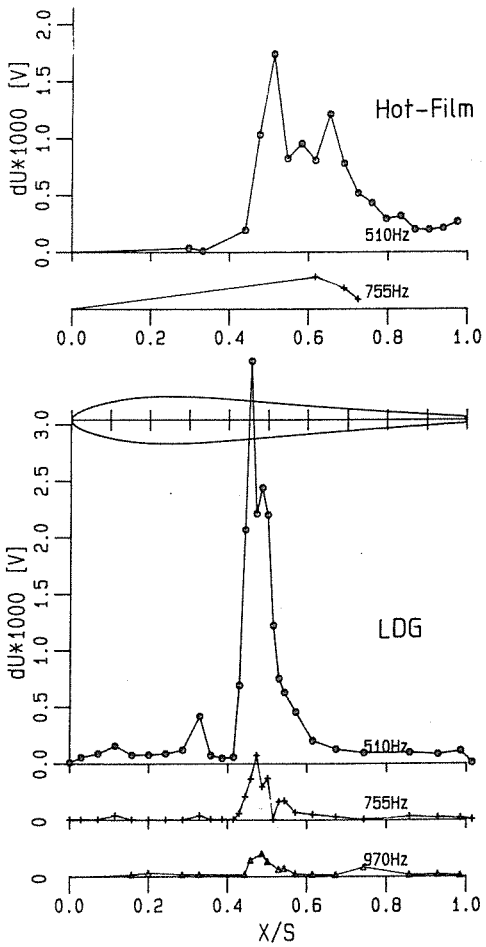

Fig. 18: Comparision of the Frequency- Spectras out of Hot-Film Measurements with LDG Measurements at Ma_t = 0.738 and α = 2°

The amplitudes of these frequencies were measured and plotted along the chord in Figs. 17 and 18. For the test case with zero incidence (Fig. 17), the hot-film sensors show periodic signals from 25% to 30% chord at the same locations where the RMS- voltages (Fig. 15) become maximal. The LDG measurements show a second maximum of periodic unsteadiness from 35% to 40% chord. Here the periodic shock motion reaches its most downstream location (compare the Schlieren picture in Fig. 15). For the higher loaded test case (α = 2°, Fig. 18), the 510 Hz frequency is dominant. No higher frequencies could be detected with hot-film measurements, and only small periodic signals were detected by LDG measurements at 755 Hz and 970 Hz. Both techniques indicate the highest periodic activities at 45% chord. The Schlieren photo (Fig. 16) here shows a strong shock and a second maximum of the periodic signal like in the zero incidence case does not exist. The LDG measurements, in general, give a more prease indication for the shock oscillation, but the hot-films provide additional data about the state of the profile boundary layer.

Conclusions

A shock system results in an increase of the RMS-voltage of the hot-film sensors. In the frequency domain, the shock is visible as a broad band frequency amplification. The time averaged DC- voltage of the hot-film sensor provides only ambigous information, and it is not recommended to rely on these signals.
The characteristic frequency of the shock is visible in the real-time data, and by this it is possible to distinguish the signals resulting from shocks from those of transitional boundary layers.
The laminar separation bubble can be detected by the RMS-output signal of the hot-film sensors, but its interpretation should be aided by additional information from other measurement techniques. In this sense, the steady state pressure distribution is very helpful. Hot-film output signals, which are typical for the laminar-turbulent transition in low speed flow could not be found.in this type of transonic flow. Here, those signals are superimposed by the signals from the shock system.
The investigation of the real-time data does not give additonal information to those already obtained by the analysis of the RMS-signals and the frequency spectra. But the real-time signal can be used very well to control the shock location during the data aquisition, if the hot-film anemomenter is connected to an oscilloscope.

References:

Broichhausen K.D., Henne J.M., Gallus H.E. 1983
"Development of Laser-Density-Gradient Technique for the Measurement of Unsteady Flow Phenomena"
Proceedings of 7th Symposiumn on Measuring Techniques and Supersonic Flow in Cascade and Turbomachines, Aachen 1983

Delery J., Marvin J.G. 1986
"Shock Wave Boundary Layer Interactions"
AGRADograph No. 280, 1986

Drees U.
"Ein Beitrag zur Dichtegradientenmessung in Überschallströmungen mit Hilfe eines quantitativen Laser-Schlierensystemes"
Dissertation RWTH Aachen 1981

Henne J.M. 1988
"Instationäre Stoß- und Grenzschichtphänomene an Einzelprofilen und in einem ebenen Gitter bei transsonischer Strömung"
Disseratation RWTH Aachen 1989

McNally, W.D., 1970
"Fortran Program for Calculating Compressible Laminar and Turbulent Boundary Layers in Arbitrary Pressure Gradients"
NASA TN D-5681

Roberts, W.B., 1975
"The Effect of Reynolds Number and Laminar Separation on Axial Cascade Performance"
Journal of Eng. For Power, Vol 97, Serie A, Nr. 2

Schroeder T. 1989
"Measurements with Hot-Film Probes and Surface-Mounted Hot-Film Gauges in a Multistage Low-Pressure Turbine"
1989 European Propulsion Forum on Modern Techniques and Developments in Engine and Component Testing, Bath

Schulz, H.D., Gallus H.E., 1989
"Experimental Investigations of the Influence of Rotor Wakes on the Development of the Profile Boundary Layer and the Performance of an Annular Compressor Cascade"
AGARD CPP-468/469, Conference on Unsteady Aerodynamic Phenomena in Turbomachines, Luxenbourg